# Apatinib, an Inhibitor of Vascular Endothelial Growth Factor Receptor 2, Suppresses Pathologic Ocular Neovascularization in Mice

Koung Li Kim and Wonhee Suh

College of Pharmacy, Chung-Ang University, Seoul, Korea

**PURPOSE.** Vascular endothelial growth factor (VEGF) signaling via VEGF receptor 2 (VEGFR2) plays a crucial role in pathologic ocular neovascularization. In this study, we investigated the antiangiogenic effect of apatinib, a pharmacologic inhibitor of VEGFR2 tyrosine kinase, against oxygen-induced retinopathy (OIR) and laser-induced choroidal neovascularization (CNV) in mice.

**METHODS.** Western blotting and in vitro angiogenesis assays were performed using human retinal microvascular endothelial cells (HRMECs). OIR was induced in neonatal mice by exposure to 75% oxygen from postnatal day (P) 7 to P12 and to room air from P12 to P17. Experimental CNV was induced in mice using laser photocoagulation. Apatinib was intravitreally and orally administered to mice. Neovascularization and phosphorylation of VEGFR2 were evaluated by immunofluorescence staining.

**RESULTS.** Apatinib inhibited VEGF-mediated activation of VEGFR2 signaling and substantially reduced VEGF-induced proliferation, migration, and cord formation in HRMECs. A single intravitreal injection of apatinib significantly attenuated retinal or choroidal neovascularization in mice with OIR or laser injury–induced CNV, respectively. Retinal or choroidal tissues of the eyes treated with apatinib exhibited substantially lower phosphorylation of VEGFR2 than those of controls injected with vehicle. Intravitreal injection of apatinib did not cause noticeable ocular toxicity. Moreover, oral administration of apatinib significantly reduced laser-induced CNV in mice.

**CONCLUSIONS.** Our study demonstrates that apatinib inhibits pathologic ocular neovascularization in mice with OIR or laser-induced CNV. Apatinib may, therefore, be a promising drug for the prevention and treatment of ischemia-induced proliferative retinopathy and neovascular age-related macular degeneration.

Keywords: apatinib, choroidal neovascularization, oxygen-induced retinopathy, receptor tyrosine kinase inhibitor, vascular endothelial growth factor

Ocular neovascularization, a major pathologic feature of blinding eye diseases, is categorized into two types depending on the tissue where it occurs.[1] In the retina, tissue ischemia triggers neovascularization by upregulating various angiogenic growth factors. The retinal vasculature becomes highly proliferative and permeable, leading to intraocular hemorrhage, retinal detachment, and severe vision loss. Retinal neovascularization is commonly seen in retinopathy of prematurity (ROP) and proliferative diabetic retinopathy (PDR). Neovascularization also occurs in subretinal or choroidal tissues in the outer retina and Bruch's membrane. The most prevalent neovascularization of this kind is neovascular age-related macular degeneration (AMD). Under normal conditions, the choriocapillaris provides sufficient blood to the retinal pigmented epithelium (RPE) that supports photoreceptor cell survival and function. However, the abnormal outgrowth of new vessels from the choriocapillaris and edema in the surrounding tissue induce detachment of the RPE from the choroid, fibrotic scarring, and vision loss.

Although the pathogenesis of ocular neovascularization is undoubtedly complex, many experimental and clinical studies have reported that vascular endothelial growth factor (VEGF) is a key mediator in the pathogenesis of intraocular disease with neovascularization.[2] VEGF regulates endothelial cell function by binding to three VEGF receptors (VEGFR): VEGFR1, VEGFR2, and VEGFR3. Among these receptors, VEGFR2, which is mainly expressed on endothelial cells, is responsible for mediating the angiogenic effects of VEGF.[3] Upon binding to VEGF, VEGFR2 becomes autophosphorylated on cytoplasmic tyrosine residues, which promote tyrosine phosphorylation of several signal transduction proteins, thereby triggering the downstream signaling pathway of VEGF-induced endothelial cell proliferation, migration, and morphogenesis. Therefore, inhibition of the VEGF signaling pathway using VEGFR2 tyrosine kinase inhibitors has emerged as a promising therapeutic strategy to reduce excessive neovascularization in several diseases.

In the present study, we explored whether apatinib, a potent and selective small-molecule inhibitor of VEGFR2 tyrosine kinase, has therapeutic potential in pathologic ocular neovascularization. Apatinib is a novel inhibitor targeting the intracellular adenosine triphosphate binding site of VEGFR2

tyrosine kinase, potently blocking the phosphorylation of VEGFR2 and subsequent downstream signaling pathways responsible for the biological effects of VEGF.[4] In preclinical experiments using several human tumor xenograft models, apatinib effectively inhibited tumor-induced angiogenesis and decreased tumor growth with little systemic toxicity.[5] A recent clinical trial report revealed that apatinib improved the progression-free survival and overall survival in patients with chemotherapy-refractory advanced metastatic gastric cancers.[6] In this regard, we propose that apatinib is also beneficial in inhibiting pathologic ocular neovascularization. In this study, we evaluated the inhibitory action of apatinib on VEGF-induced angiogenesis using in vitro assays with human retinal microvascular endothelial cells (HRMECs). We also investigated the in vivo therapeutic action of apatinib against mouse models of oxygen-induced retinopathy (OIR) and laser-induced choroidal neovascularization (CNV), which mimic ROP and neovascular AMD, respectively.

## METHODS

### Cell Culture

In vitro studies were performed using HRMECs (Cell Systems, Kirkland, WA, USA) at passages 3 to 6. The cells were cultured in endothelial growth medium-2 (Lonza, Walkersville, MD, USA) at 37°C under a humidified 95%:5% (vol/vol) mixture of air and $CO_2$.[7]

### Western Blotting

Cells were lysed in ice-cold lysis buffer containing protease/phosphatase inhibitor cocktail (Cell Signaling Technology, Danvers, MA, USA). Cell lysates were separated using sodium dodecyl sulfate-polyacrylamide gel electrophoresis. The blots were incubated with the appropriate primary IgGs: phospho-VEGFR2 (p-VEGFR2; Origene, Rockville, MD, USA), phospho-extracellular signal–regulated kinase (p-ERK; R&D Systems, Minneapolis, MN, USA), VEGFR2 (R&D Systems), ERK (Cell Signaling Technology), and β-actin (Sigma-Aldrich Corp., St. Louis, MO, USA), followed by horseradish peroxidase–conjugated secondary IgGs. Immunoreactive bands were then visualized with a chemiluminescent reagent (Amersham Biosciences, Piscataway, NJ, USA).

### In Vitro Angiogenesis Assays

For the analysis of the inhibitory effects of apatinib (MWt = 493 Da; LSK Biopharma, Salt Lake City, UT, USA) on angiogenesis induced by recombinant human VEGF165 (rhVEGF; R&D Systems), recombinant human platelet-derived growth factor-BB (rhPDGF-BB; R&D Systems), and recombinant human basic fibroblast growth factor (rhbFGF; R&D Systems), cord formation, scratch wounding migration, and cell proliferation assays were performed as previously described.[8] In the cord formation assay, cells ($3 \times 10^4$/well) were seeded onto Matrigel (BD Bioscience, Bedford, MA, USA)–coated 24-well plates and treated with endothelial basal medium (EBM; Lonza) containing 1% fetal bovine serum (FBS; Lonza), or supplemented with angiogenic growth factor (100 ng/mL rhVEGF, 20 ng/mL rhPDGF-BB, or 20 ng/mL rhbFGF) and/or apatinib (1 μM). After incubation for 6 hours, cord networks were quantified by measuring cord lengths in four random microscope fields. In order to analyze scratch wounding migration, confluent cell monolayers grown in gelatin-coated six-well plates were scratched using pipette tips and washed with phosphate-buffered saline (PBS). Cells were then incubated with EBM

containing 1% FBS, or supplemented with angiogenic growth factor and/or apatinib (1 μM) for 24 hours. Cell migration was observed by microscopy and quantified by measuring the area covered by the cells that had migrated from the wound edges. In the cell proliferation assay, cells ($1 \times 10^4$/well) were seeded in gelatin-coated 96-well plates and incubated with EBM containing 1% FBS or supplemented with angiogenic growth factor and/or apatinib (1 μM) for 3 days. Cell proliferation was assessed using a Cell Counting Kit-8 (CCK-8; Dojindo Molecular Technology, Inc., Rockville, MD, USA) or Ki67 immunofluorescence assays. In the CCK-8 assay, 10 μL CCK-8 solution was added to each well, and the 96-well plate was incubated at 37°C for 4 hours. The absorbance at 450 nm of each well was then read using a microplate reader (BioTek Instruments, Seoul, Korea) to determine the number of viable cells. In the Ki67 immunofluorescence assay, cells were stained with anti-Ki67 IgG (R&D Systems). Five representative color images were randomly acquired from each sample to quantify Ki67+ cells, and the ratio of Ki67+ cells was calculated by dividing the number of Ki67+ cells by the total number of cells in a given image.

### Animals

Procedures involving animals were approved by the Institutional Animal Care and Use Committee in accordance with the ARVO Statement for the Use of Animals in Ophthalmic and Vision Research. Nine- to ten-week-old male or pregnant C57BL/6 mice were purchased from Orient Co., Ltd. (Seoul, Korea). Mice were anesthetized with an intraperitoneal injection of ketamine (79.5 mg/kg) and xylazine (9.1 mg/kg). The pupils of anesthetized mice were dilated with topical 1% tropicamide (Santen, Osaka, Japan).

### Mouse Model of OIR

OIR was induced in mice using the protocol reported by Smith et al.[9] Briefly, litters of newborn mice and their nursing mothers were exposed to 75% oxygen from postnatal day (P) 7 to P12 in an acrylic chamber connected to an oxygen controller (ProOx P110; BioSpherix, Parish, NY, USA). On P12, the mice were returned to the environment with normal oxygen content and received a single intravitreal injection of 1 μL apatinib solution (2 mM in dimethyl sulfoxide [DMSO]) or an equivalent volume of DMSO (contralateral control). On P17, after 5 days of exposure to normoxia, the mice were euthanized, and both eyes were harvested for the analysis of retinal neovascularization.

### Quantification of Retinal Neovascularization

The eyes were enucleated and fixed overnight in 4% paraformaldehyde. Retinas were dissected, soaked in blocking solution (5% bovine serum albumin, 5% normal donkey serum, 0.5% Triton X-100 in PBS), and then stained with Alexa Fluor 594–conjugated *Griffonia Simplicifolia* isolectin B4 (1:100 dilution; Invitrogen, Carlsbad, CA, USA) in PBS containing 1 mM $CaCl_2$ overnight at 4°C. The next day, the retinas were washed twice with PBS, flat-mounted on microscope slides, and embedded in fluorescence mounting medium (Dako, Carpinteria, CA, USA). Immunofluorescence images of the entire retina were obtained using a fluorescence microscope (Olympus, Tokyo, Japan). In each whole mount, the number of pixels in the neovascular tufts was measured using ImageJ software (National Institutes of Health, Bethesda, MD, USA) and compared to the total number of pixels in the entire retina.[10]
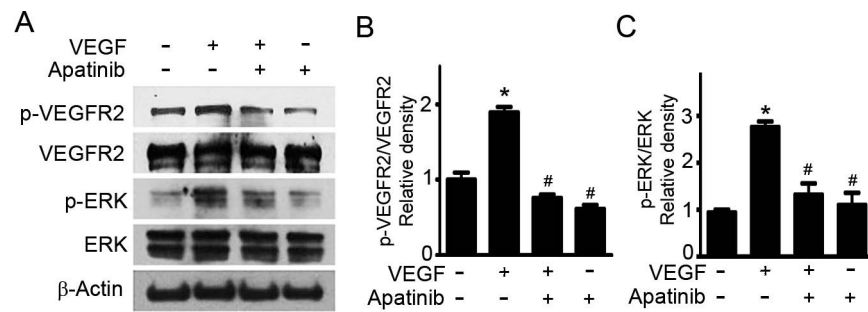
**FIGURE 1.** Apatinib inhibits VEGF-induced phosphorylation of VEGFR2 and ERK in HRMECs. (**A**) Representative Western blotting images and (**B**, **C**) densitometric analysis of phosphorylated VEGFR2 (p-VEGFR2; B) and phosphorylated ERK (p-ERK; C) are illustrated. HRMECs treated with apatinib (1 μM) and untreated cells were stimulated with rhVEGF (100 ng/mL) or PBS for 20 minutes. Cell lysates were subjected to Western blotting using primary IgGs against p-VEGFR2 and p-ERK. The membranes were then stripped and reprobed with IgGs against VEGFR2, ERK, and β-actin. Band intensities of p-VEGFR2 and p-ERK were normalized to the band intensities of VEGFR2 and ERK, respectively (*$P < 0.05$ versus PBS, #$P < 0.05$ versus VEGF only, $n = 3$).

## Mouse Model of Laser-Induced CNV

Nine- to ten-week-old male C57BL/6 mice were used as subjects for laser-induced CNV.[11] Immediately after anesthesia and pupil dilation, experimental CNV lesions (four spots per eye) were created between major retinal vessels adjacent to the optic nerve by laser photocoagulation (532 nm; IRIS Medical, Mountain View, CA, USA) set to the 75-μm spot size, 130-mW intensity, and 0.1-second duration. Only mice with cavitation bubbles, which indicated the disruption of Bruch's membrane, were included in the study. Immediately after CNV induction, the anesthetized mice received a single intravitreal injection of 1 μL apatinib solution (2 mM in DMSO) or an equivalent volume of DMSO (contralateral control). Two weeks later, the mice were euthanized for further analysis. For the oral administration experiment, apatinib was suspended in solution containing 0.5% carboxymethylcellulose (CMC) (Sigma-Aldrich Corp.) and 5% glucose, and mice received oral gavage (once daily) of apatinib suspension (100 or 200 mg/kg per day) or an equivalent volume of solution containing 0.5% CMC and 5% glucose. Oral gavage started on the day of CNV development and continued for 2 weeks before quantification of the CNV lesion area.

## Quantification of Laser-Induced CNV

The eyes were enucleated and fixed in 4% paraformaldehyde solution in PBS. The posterior eyecups comprising the RPE, choroid, and sclera were microdissected from the surrounding tissues and prepared as flat mounts. The flat mounts were then soaked in blocking solution and stained with Alexa Fluor 594–conjugated isolectin B4 (1:100 dilution; Invitrogen) overnight at 4°C. Images of CNV lesions were obtained using a fluorescence microscope (Olympus), and the fluorescence intensity of each image was analyzed using ImageJ software (National Institutes of Health).[11]

## Immunohistochemistry

The eyes were enucleated, fixed, and embedded in OCT compound (Sakura Finetek, Torrance, CA, USA) or paraffin. After quenching endogenous peroxidase activity and blocking with 10% normal goat serum, tissue sections were incubated with primary IgGs against p-VEGFR2 (Origene) or glial fibrillary acidic protein (GFAP; Dako), and then incubated with the appropriate fluorescent secondary IgG. Blood vasculature was visualized by costaining with Alexa Fluor 594–conjugated isolectin B4 (Invitrogen). Cell nuclei were stained with 4,6-diamidino-2-phenylindole (DAPI; Vector Laboratories, Burlingame, CA, USA). Images were obtained using a fluorescence microscope (Olympus), and the number of sections examined ranged from six to eight per group.

## Histologic Analysis

Hematoxylin and eosin (H&E) staining was performed on paraffin sections. Retinal thickness was assessed by calculating the ratio of A (the distance from the ganglion cell layer to the outer edge of the inner nuclear layer) to B (the distance from the ganglion cell layer to the outer edge of the outer nuclear layer).[12]

## Terminal Deoxynucleotidyl Transferase dUTP Nick End-Labeling (TUNEL) Assay

TUNEL assays were performed on paraffin sections using the In Situ Cell Death Detection Kit (Roche Applied Science, Mannheim, Germany) according to the manufacturer's instructions. Counterstaining for total nuclei was performed by mounting with antifade medium containing DAPI (Vector Laboratories). As a positive control, paraffin sections were treated with DNase I (1500 U/mL, Roche Applied Science) for 10 minutes at room temperature to induce DNA strand breaks. Images were obtained using a fluorescence microscope (Olympus). Six to ten sections were examined per group.

## Statistical Analysis

All data are expressed as the mean ± standard error of mean (SEM) of indicated $n$ values. One-way analysis of variance was used to determine the significance of differences between groups. Where appropriate, data were analyzed using post hoc Student's $t$-tests for unpaired observations and the Bonferroni correction for multiple comparisons. Differences were considered significant when $P < 0.05$.

## RESULTS

### Apatinib Inhibits VEGF-Induced Angiogenic Activity in HRMECs

Apatinib up to 5 μM did not induce cytotoxicity in HRMECs (data not shown). We then evaluated the inhibitory effect of apatinib on VEGF-induced activation of the VEGFR2 signaling pathway and the angiogenic response in HRMECs. Western blotting analysis showed that VEGFR2 and ERK were substantially phosphorylated within 20 minutes after exposure to VEGF (Fig. 1). Pretreatment with apatinib (1 μM) significantly
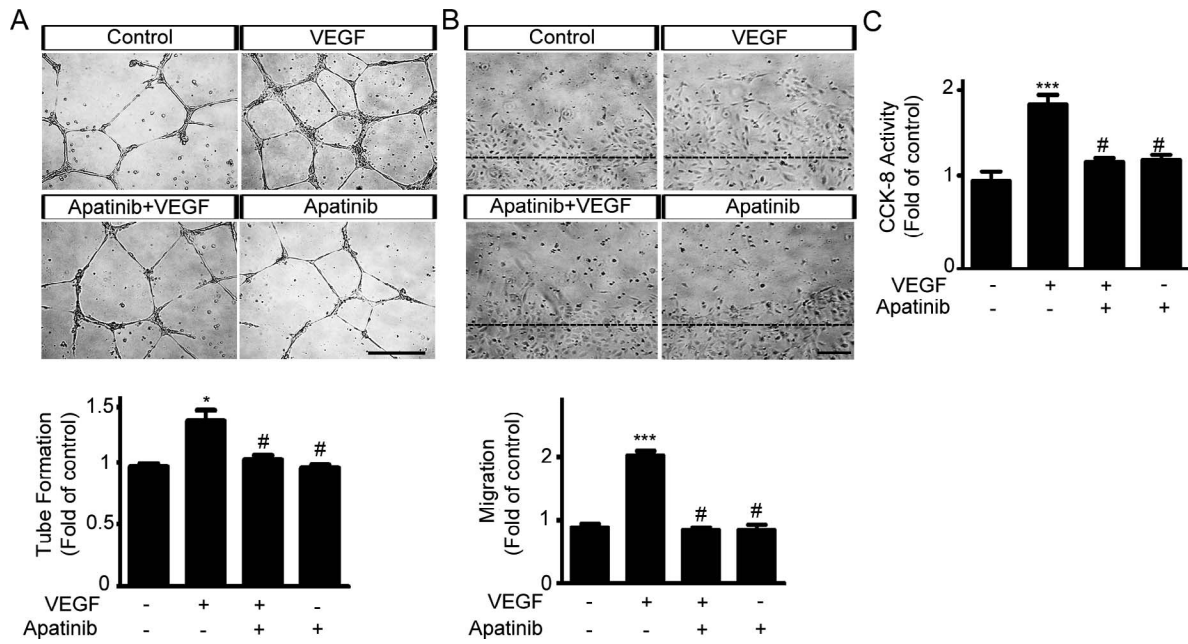
**FIGURE 2.** Apatinib decreases VEGF-induced angiogenic activity of HRMECs. Apatinib inhibits VEGF-induced increases in (**A**) cord formation, (**B**) scratch wounding migration, and (**C**) cell proliferation of HRMECs. HRMECs treated with apatinib (1 µM) and untreated cells were incubated with rhVEGF (100 ng/mL) or PBS. All data were normalized to the values of the corresponding controls. Cord formation and scratch wounding migration were quantified by measuring the cord length and relative area covered by cells that had migrated from the wound edges (*black dashed lines*), respectively. Cell proliferation was analyzed using the CCK-8 assay. Data are presented as the mean ± SEM (*$P < 0.05$, ***$P < 0.001$ versus PBS, #$P < 0.05$ versus VEGF only, $n = 6$). *Scale bars*: 200 µm.
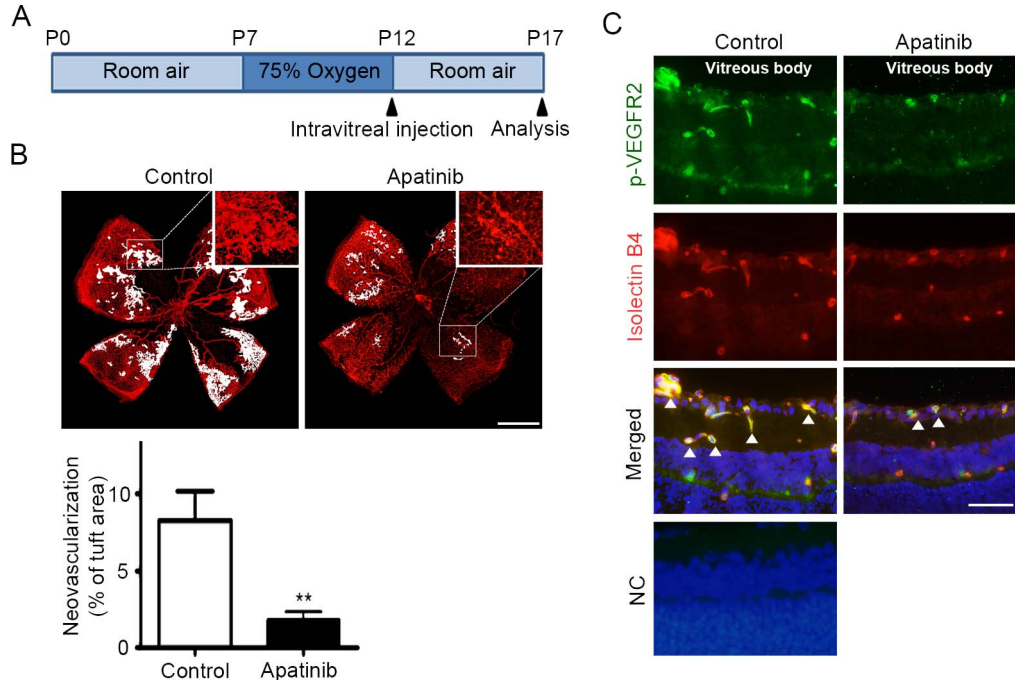


**FIGURE 3.** Intravitreal injection of apatinib decreases retinal neovascularization in mice with OIR. (**A**) Schematic diagram of the OIR experiment. On P12, mice received a single intravitreal injection of apatinib (1 µg in 1 µL DMSO) or DMSO (1 µL; contralateral control). Five days later (on P17), the eyes were harvested for further analysis. (**B**) Representative images of whole-mounted retinas with neovascular tufts highlighted in *white*, and quantification of retinal neovascularization. Retinal vasculature was visualized by staining with isolectin B4 (*red*). The extent of retinal neovascularization was calculated by dividing the number of pixels in the neovascular tuft area by the number of pixels in the total retinal area. All data are presented as the mean ± SEM (**$P < 0.01$, $n = 4$ mice per group). *Scale bar*: 500 µm. (**C**) Immunofluorescence staining was performed using anti-p-VEGFR2 IgGs (*green*) and isolectin B4 (*red*) on cryosections prepared from the eyecups of mice with OIR. The *arrowheads* indicate the double labeling of p-VEGFR2 and isolectin B4. Sections stained with irrelevant nonspecific IgGs are included as negative controls (NC). The nuclei are shown in *blue* (DAPI). Representative images were selected from three independent experiments with similar results. *Scale bar*: 50 µm.
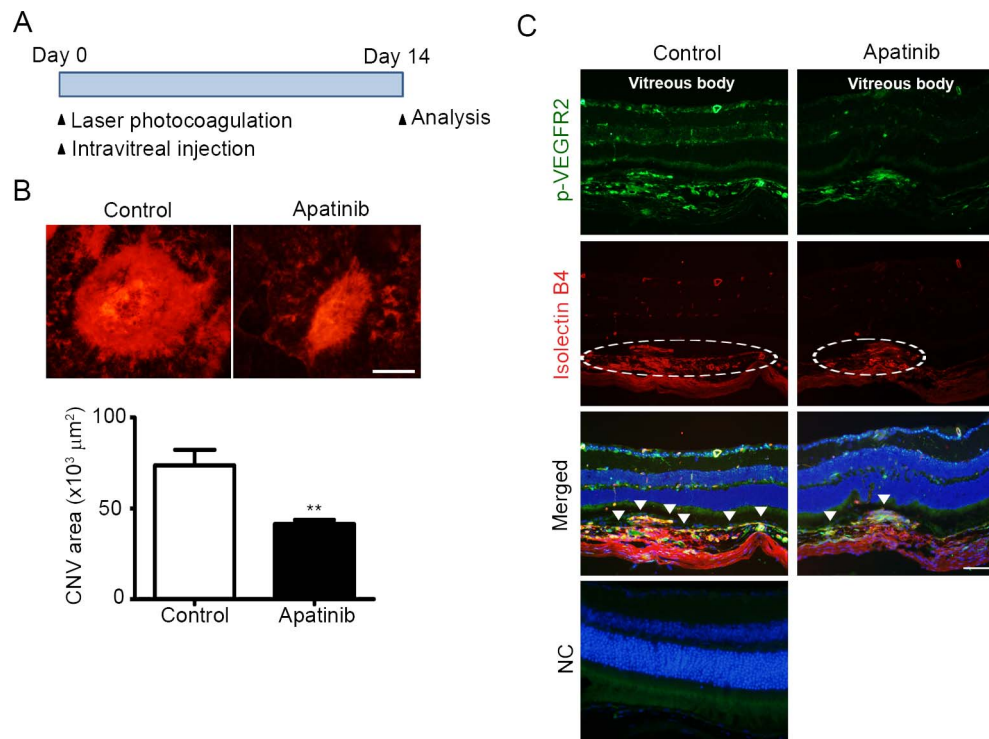
**FIGURE 4.** Intravitreal injection of apatinib decreases CNV formation in mice with laser-induced CNV. (**A**) Schematic diagram of the laser-induced CNV experiment. Immediately after laser photocoagulation, mice received a single intravitreal injection of apatinib (1 μg in 1 μL DMSO) or DMSO (1 μL; contralateral control). Two weeks later, the eyes were harvested for further analysis. (**B**) Representative images of flat-mounted choroids with CNV and quantification of the isolectin B4–positive CNV area. The posterior eyecups composed of RPE, choroid, and sclera were flat-mounted and stained with isolectin B4 (*red*). The CNV areas were quantified by measuring the fluorescence intensity of images with isolectin B4–positive areas. All data are presented as the mean $\pm$ SEM (**$P < 0.01$, $n = 4$ mice per group). (**C**) Immunofluorescence staining was performed using anti-p-VEGFR2 IgGs (*green*) and isolectin B4 (*red*) on cryosections prepared from the eyecups of mice with CNV. The *arrowheads* indicate the double labeling of p-VEGFR2 and isolectin B4 in CNV lesions (*white dashed circles*). Sections stained with irrelevant nonspecific IgGs are included as negative controls (NC). The nuclei are shown in *blue* (DAPI). Representative images were selected from three independent experiments with similar results. *Scale bars*: 100 μm.

reduced VEGF-induced phosphorylation of VEGFR2 and ERK. Because angiogenesis involves various coordinated events, including proliferation, migration, and morphogenesis of endothelial cells, we performed three different in vitro angiogenesis assays including Matrigel cord formation, scratch wounding migration, and cell proliferation quantified by the CCK-8 assay. Figure 2 shows that VEGF significantly increased cord formation, migration, and proliferation of HRMECs. Cotreatment with apatinib (1 μM) completely inhibited VEGF-induced angiogenic manifestations in HRMECs. However, treatment with apatinib had no significant effect on the angiogenic activity of HRMECs in response to bFGF or PDGF-BB (Supplementary Figs. S1, S2). These results indicate that apatinib efficiently and selectively inhibits VEGF-induced angiogenesis in HRMECs.

## Intravitreal Injection of Apatinib Decreases Retinal Neovascularization in Mice With OIR

To determine the effect of apatinib on pathologic retinal neovascularization, we used OIR, a well-established animal model of ischemia-induced retinal neovascularization. Newborn mice were exposed to 75% oxygen from P7 to P12. On P12, they were returned to a normoxic environment and were intravitreally administered apatinib or DMSO. On P17, the extent of neovascularization was determined by measuring the formation of neovascular tufts that reflected pathologic retinal neovascularization (Fig. 3A). While the DMSO-treated contra-

lateral control eyes exhibited pronounced retinal neovascularization (tuft formation), the apatinib-treated eyes showed markedly reduced neovascularization (Fig. 3B). Quantitative analysis showed that the neovascularization area in mice treated with apatinib and DMSO comprised $1.85 \pm 0.50\%$ and $8.34 \pm 1.91\%$ of the total retinal area, respectively. Thus, in the apatinib-treated group, ischemia-induced pathologic retinal neovascularization was 77.82% lower than that in the DMSO-treated control group. Furthermore, we performed immunohistochemical staining of retinal transverse sections in order to assess whether intravitreally injected apatinib could reduce the phosphorylation of VEGFR2. Figure 3C shows a substantial decrease of p-VEGFR2 signal in the isolectin B4–positive endothelial cells in retinal sections of the apatinib-injected eyes compared to the strong p-VEGFR2 signal in the cells of the DMSO-injected eyes.

## Intravitreal Injection of Apatinib Decreases CNV Formation in Mice With Laser-Induced CNV

To determine the effect of apatinib on pathologic CNV, we employed a common CNV mouse model, where laser-induced injury ruptures the Bruch's membrane, resulting in the growth of new vessels from the choroid into the subretinal space. Immediately after laser photocoagulation, apatinib or DMSO was intravitreally injected into mice. Two weeks later, the areas of CNV lesions were evaluated (Fig. 4A). Representative images of the isolectin B4–stained CNV lesions show
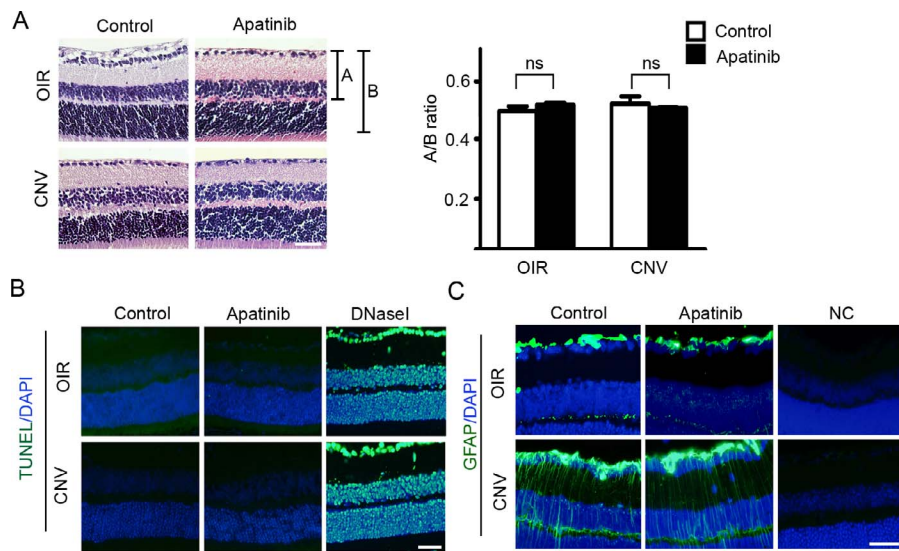
**FIGURE 5.** Intravitreal injection of apatinib does not induce ocular toxicity. As described in the previous experiments for the prevention of OIR and CNV, mice received a single intravitreal injection of apatinib (1 μg in 1 μL DMSO) or DMSO (1 μL; contralateral control) on P12 or immediately after laser injury. The eyes were harvested on P17 or 2 weeks after laser injury. Note that the retinal toxicity of apatinib in mice with CNV was assessed in the regions without CNV lesions. (**A**) Representative H&E-stained images of retinas and quantification of the ratio of A (the distance from the ganglion cell layer to the outer edge of the inner nuclear layer) to B (the distance from the ganglion cell layer to the outer edge of the outer nuclear layer). Data are presented as the mean ± SEM (ns, not significant; $n = 4$ mice per group). (**B**) TUNEL assay and (**C**) immunofluorescence staining with anti-GFAP IgG were performed on paraffin sections. In the TUNEL assay, DNase I–treated sections were included as positive controls. In the immunofluorescence staining with anti-GFAP IgG, sections stained with irrelevant nonspecific IgGs were included as negative controls (NC). The nuclei are shown in *blue* (DAPI). Representative images in (**B**) and (**C**) were selected from three independent experiments with similar results. *Scale bars*: 50 μm.

that the areas of CNV lesions in apatinib-treated mice were much smaller than those in DMSO-treated controls (Fig. 4B). Quantitative analysis showed that the areas of CNV lesions in mice treated with apatinib and DMSO were $41.35 \pm 2.39 \times 10^3$ and $73.68 \pm 8.73 \times 10^3$ μm², respectively. Therefore, the mean area of CNV lesions was 43.88% lower in the apatinib-treated group than that in the DMSO-treated control group. In addition, the immunohistochemical analysis of tissue sections showed that the apatinib-injected eyes exhibited much lower p-VEGFR2 signal in isolectin B4–positive endothelial cells in CNV lesions than DMSO-injected contralateral controls did (Fig. 4C).

## Intravitreal Injection of Apatinib Does Not Induce Retinal Toxicity in Mice

To assess whether intravitreal injection of apatinib causes retinal toxicity in mice with OIR or CNV, we performed histologic examinations, TUNEL assays, and anti-GFAP immunohistochemistry on retinal sections that were obtained from the previous experiments shown in Figures 3 and 4. Examination of H&E-stained retinal sections and quantification of retinal thickness revealed no change in histologic morphology or retinal thickness between the apatinib-treated eyes and DMSO controls (Fig. 5A). In addition, retinal sections were stained for GFAP and TUNEL to assess any retinal toxicity or apoptosis. In mice with OIR, intravitreal injection of apatinib did not increase TUNEL-positive cells and GFAP expression compared to what was observed with DMSO injection (Figs. 5B, 5C). In mice with CNV, examination of retinal tissues with no lesions revealed no difference in apoptosis and GFAP expression between the apatinib-treated eyes and DMSO controls (Figs. 5B, 5C). These data suggest the absence of intraocular toxicity of apatinib in mice with OIR or CNV.
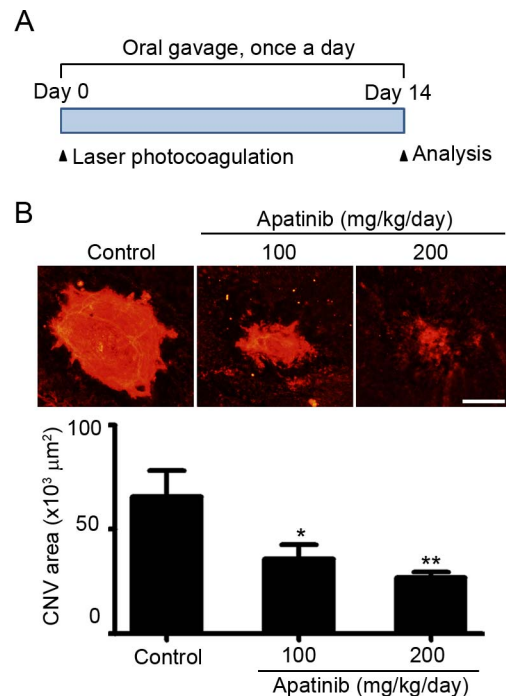


**FIGURE 6.** Oral administration of apatinib reduces laser-induced CNV formation in mice. (**A**) Schematic diagram of the laser-induced CNV experiment. Mice received oral gavage (once a day) of apatinib suspension (100 or 200 mg/kg per day) or an equivalent volume of vehicle (Control). Oral gavage was started on the day of CNV induction and continued for 2 weeks before analysis. (**B**) Representative images of flat-mounted choroids with CNV and quantification of the isolectin B4–positive CNV area. The CNV area was quantified by measuring the red fluorescence intensity of the isolectin B4–positive area. All data are presented as the mean ± SEM (*$P < 0.05$, **$P < 0.01$, $n = 5$ mice per group). *Scale bar*: 100 μm.

### Oral Administration of Apatinib Reduces Laser-Induced CNV Formation in Mice

Since VEGFR2 is present in the retinal vascular endothelium, which is easily accessible to drugs circulating in the blood, and apatinib is an orally bioavailable drug, we hypothesized that oral administration of apatinib would inhibit laser-induced CNV. Starting from the day of CNV development, mice received oral gavage of apatinib once daily for 14 days (Fig. 6A). The doses of apatinib were selected based on the therapeutic doses utilized in human tumor xenograft experiments.[5] Quantitative analysis of the areas of CNV lesions showed that oral administration of apatinib significantly inhibited CNV formation in a dose-dependent manner (Fig. 6B). The areas of CNV lesions in mice treated with 100 and 200 mg/kg per day of apatinib were $35.92 \pm 6.99 \times 10^3$ and $26.84 \pm 2.80 \times 10^3$ $\mu m^2$, respectively. When compared to that of the control group, mice treated with 100 and 200 mg/kg per day of apatinib exhibited a 45.18% and 59.04% decrease in the area of CNV lesions, respectively.

## DISCUSSION

Retinal and choroidal neovascularization are the major causes of blindness in several eye diseases, such as neovascular AMD, ROP, and PDR, which cause a significant health and economic burden. Many previous studies have indicated that pathologic transformations of the retinal and choroidal vasculature are strongly associated with increased expression of VEGF-A. In humans, the expression levels of VEGF-A were significantly higher in patients with PDR, ROP, and CNV secondary to AMD.[13-15] Patients with pronounced retinal neovascularization were likely to have higher ocular expression of VEGF-A than patients without neovascular pathologic features.[16] In animal models, the expression levels of VEGF-A were temporally and spatially correlated with the severity of neovascularization.[17] Moreover, anti-VEGF-A therapy efficiently decreased retinal and choroidal neovascularization in animal models.[18,19] These preclinical data have been confirmed in large multicenter clinical trials of patients with neovascular AMD.[20,21] In addition to VEGF-A, other members of the VEGF family may also contribute to pathologic ocular neovascularization. Immuno-histochemical analysis showed that VEGF-C and VEGF-D were highly expressed in the RPE and vascular cells in the subretinal and choroidal neovascular membranes of AMD patients.[22,23] A recent study also reported that VEGF-C and VEGF-D protein levels were elevated in the vitreous fluids of patients with AMD.[22] In a profiling study of angiogenic and inflammatory vitreous markers, the vitreous levels of VEGF-C and VEGF-D were much higher in patients with PDR or neovascular glaucoma than in nondiabetic control patients.[24] In a mouse model of this condition, the expression levels of VEGF-C and VEGF-D were higher than those in normal animals (Lashkari K, et al. *IOVS* 2013:ARVO E-Abstract 4999). Since VEGF-C and VEGF-D not only modulate lymphangiogenesis by activating VEGFR3, but also enhance angiogenesis by phosphorylating VEGFR2, it is likely that VEGF-C and VEGF-D contribute to pathologic ocular neovascularization.[25-27] Therefore, inhibition of VEGFR2, a common angiogenic signal transducer of VEGF-A, -B, and -C, may be an attractive therapeutic strategy for the treatment of intraocular diseases that involve neovascularization.

Apatinib is a novel receptor tyrosine kinase inhibitor that selectively targets VEGFR2.[5] Since angiogenesis is important in the development and progression of cancer, apatinib was initially developed as an anticancer drug and is currently being studied as a third-line treatment option for advanced metastatic gastric cancer.[4] A recent study revealed that apatinib exerted potent antitumor effects with tolerable and clinically manageable toxicity in patients with chemotherapy-refractory gastric cancers.[6] In the present study, we demonstrated the pharmacologic activity and safety of apatinib in the context of pathologic ocular neovascularization. Apatinib exhibited a potent inhibitory action on VEGF-induced proliferation, migration, and cord formation of HRMECs. In mice with OIR or laser-induced CNV, a single intravitreal injection of apatinib inhibited the phosphorylation of VEGFR2 and significantly suppressed ocular neovascularization without retinal toxicity. Considering the small vitreous volume of a mouse, a very high dose of apatinib was administered to the mice in the present study. However, the poor water solubility of apatinib would cause apatinib to immediately precipitate to form a depot in the vitreous humor after the intravitreal injection. Then, the precipitated drug would slowly dissolve to give a vitreous concentration near its aqueous solubility, which is often the case with intravitreal injections of poorly water-soluble drugs such as triamcinolone acetonide.[28] Due to its hydrophobicity and low molecular weight, apatinib is likely to be distributed in the posterior chamber rather than in the anterior chamber and would be eliminated through the blood–ocular barrier to the choroidal vasculature that constitutes most of the ocular blood flow.[29] We demonstrated that oral administration of apatinib substantially inhibited CNV formation in mice at the dose equivalent to the therapeutic dose observed in human tumor xenograft experiments. Following oral absorption, apatinib could become available in the systemic circulation and easily access the choroidal endothelium where VEGFR2 is expressed. This result suggests that the inhibitory action of apatinib on VEGFR2 does not necessitate the intravitreal injections that are required for anti-VEGF agents whose target, VEGF, is present in the vitreous cavity.

Taken together, these findings suggest repositioning of apatinib, an anticancer drug, for treatment of neovascular AMD and ischemic proliferative retinopathies such as ROP and PDR. However, it is important to note potential side effects associated with VEGFR2 inhibition during clinical applications of apatinib. Because VEGF plays crucial roles in the maintenance of vascular homeostasis, chronic and/or excessive inhibition of VEGF signaling could cause thromboembolic and hemorrhagic events.[30,31] Additional research is needed to determine optimal doses and intravitreal delivery methods for the clinical applications of apatinib.

### References

1. Campochiaro PA. Molecular pathogenesis of retinal and choroidal vascular diseases. *Prog Retin Eye Res*. 2015;49:67–81.

2. Miller JW, Le Couter J, Strauss EC, Ferrara N. Vascular endothelial growth factor a in intraocular vascular disease. *Ophthalmology*. 2013;120:106–114.

3. Koch S, Claesson-Welsh L. Signal transduction by vascular endothelial growth factor receptors. *Cold Spring Harb Perspect Med*. 2012;2:a006502.

4. Roviello G, Ravelli A, Polom K, et al. Apatinib: a novel receptor tyrosine kinase inhibitor for the treatment of gastric cancer. *Cancer Lett*. 2016;372:187–191.

Investigative Ophthalmology & Visual Science

5. Tian S, Quan H, Xie C, et al. YN968D1 is a novel and selective inhibitor of vascular endothelial growth factor receptor-2 tyrosine kinase with potent activity in vitro and in vivo. *Cancer Sci*. 2011;102:1374–1380.

6. Li J, Qin S, Xu J, et al. Apatinib for chemotherapy-refractory advanced metastatic gastric cancer: results from a randomized, placebo-controlled, parallel-arm, phase II trial. *J Clin Oncol*. 2013;31:3219–3225.

7. Kim SR, Suh W. Beneficial effects of the Src inhibitor, dasatinib, on breakdown of the blood-retinal barrier. *Arch Pharm Res*. 2017;40:197–203.

8. Kim KL, Meng Y, Kim JY, Baek EJ, Suh W. Direct and differential effects of stem cell factor on the neovascularization activity of endothelial progenitor cells. *Cardiovasc Res*. 2011;92:132–140.

9. Smith LE, Wesolowski E, McLellan A, et al. Oxygen-induced retinopathy in the mouse. *Invest Ophthalmol Vis Sci*. 1994;35:101–111.

10. Connor KM, Krah NM, Dennison RJ, et al. Quantification of oxygen-induced retinopathy in the mouse: a model of vessel loss, vessel regrowth and pathological angiogenesis. *Nat Protoc*. 2009;4:1565–1573.

11. Lambert V, Lecomte J, Hansen S, et al. Laser-induced choroidal neovascularization model to study age-related macular degeneration in mice. *Nat Protoc*. 2013;8:2197–2211.

12. Park SW, Kim JH, Kim KE, et al. Beta-lapachone inhibits pathological retinal neovascularization in oxygen-induced retinopathy via regulation of HIF-1alpha. *J Cell Mol Med*. 2014;18:875–884.

13. Adamis AP, Miller JW, Bernal MT, et al. Increased vascular endothelial growth factor levels in the vitreous of eyes with proliferative diabetic retinopathy. *Am J Ophthalmol*. 1994;118:445–450.

14. Grisanti S, Tatar O. The role of vascular endothelial growth factor and other endogenous interplayers in age-related macular degeneration. *Prog Retin Eye Res*. 2008;27:372–390.

15. Sato T, Kusaka S, Shimojo H, Fujikado T. Vitreous levels of erythropoietin and vascular endothelial growth factor in eyes with retinopathy of prematurity. *Ophthalmology*. 2009;116:1599–1603.

16. Aiello LP, Avery RL, Arrigg PG, et al. Vascular endothelial growth factor in ocular fluid of patients with diabetic retinopathy and other retinal disorders. *N Engl J Med*. 1994;331:1480–1487.

17. Miller JW, Adamis AP, Shima DT, et al. Vascular endothelial growth factor/vascular permeability factor is temporally and spatially correlated with ocular angiogenesis in a primate model. *Am J Pathol*. 1994;145:574–584.

18. Aiello LP, Pierce EA, Foley ED, et al. Suppression of retinal neovascularization in vivo by inhibition of vascular endothelial growth factor (VEGF) using soluble VEGF-receptor chimeric proteins. *Proc Natl Acad Sci U S A*. 1995;92:10457–10461.

19. Krzystolik MG, Afshari MA, Adamis AP, et al. Prevention of experimental choroidal neovascularization with intravitreal anti-vascular endothelial growth factor antibody fragment. *Arch Ophthalmol*. 2002;120:338–346.

20. Maguire MG, Martin DF, Ying GS, et al. Five-year outcomes with anti-vascular endothelial growth factor treatment of neovascular age-related macular degeneration: the Comparison of Age-Related Macular Degeneration Treatments Trials. *Ophthalmology*. 2016;123:1751–1761.

21. Talks JS, Lotery AJ, Ghanchi F, et al. First-year visual acuity outcomes of providing aflibercept according to the VIEW study protocol for age-related macular degeneration. *Ophthalmology*. 2016;123:337–343.

22. Ikeda Y, Yonemitsu Y, Onimaru M, et al. The regulation of vascular endothelial growth factors (VEGF-A, -C, and -D) expression in the retinal pigment epithelium. *Exp Eye Res*. 2006;83:1031–1040.

23. Otani A, Takagi H, Oh H, et al. Vascular endothelial growth factor family and receptor expression in human choroidal neovascular membranes. *Microvasc Res*. 2002;64:162–169.

24. Kovacs K, Marra KV, Yu G, et al. Angiogenic and inflammatory vitreous biomarkers associated with increasing levels of retinal ischemia. *Invest Ophthalmol Vis Sci*. 2015;56:6523–6530.

25. Achen MG, Jeltsch M, Kukk E, et al. Vascular endothelial growth factor D (VEGF-D) is a ligand for the tyrosine kinases VEGF receptor 2 (Flk1) and VEGF receptor 3 (Flt4). *Proc Natl Acad Sci U S A*. 1998;95:548–553.

26. Cao Y, Linden P, Farnebo J, et al. Vascular endothelial growth factor C induces angiogenesis in vivo. *Proc Natl Acad Sci U S A*. 1998;95:14389–14394.

27. Joukov V, Pajusola K, Kaipainen A, et al. A novel vascular endothelial growth factor, VEGF-C, is a ligand for the Flt4 (VEGFR-3) and KDR (VEGFR-2) receptor tyrosine kinases. *EMBO J*. 1996;15:1751.

28. Kamppeter BA, Cej A, Jonas JB. Intraocular concentration of triamcinolone acetonide after intravitreal injection in the rabbit eye. *Ophthalmology*. 2008;115:1372–1375.

29. del Amo EM, Vellonen KS, Kidron H, Urtti A. Intravitreal clearance and volume of distribution of compounds in rabbits: in silico prediction and pharmacokinetic simulations for drug development. *Eur J Pharm Biopharm*. 2015;95:215–226.

30. Eremina V, Jefferson JA, Kowalewska J, et al. VEGF inhibition and renal thrombotic microangiopathy. *N Engl J Med*. 2008;358:1129–1136.

31. Zangari M, Fink LM, Elice F, Zhan F, Adcock DM, Tricot GJ. Thrombotic events in patients with cancer receiving anti-angiogenesis agents. *J Clin Oncol*. 2009;27:4865–4873.

Investigative Ophthalmology & Visual Science